AAPS PharmSciTech, Vol. 14, No. 3, September 2013 (© 2013)
DOI: 10.1208/s12249-013-9988-3

Research Article

Freeze-Dried Targeted Mannosylated Selenium-Loaded Nanoliposomes: Development and Evaluation

Susanne R. Youngren,[1] Rohit Mulik,[1] Byoung Jun,[1] Peter R. Hoffmann,[2] Kenneth R. Morris,[1] and Mahavir B. Chougule[1,3]

Received 19 December 2012; accepted 28 May 2013; published online 26 June 2013

Abstract. The aim of this investigation was to develop and evaluate freeze-dried mannosylated liposomes for the targeted delivery of selenium. Dipalmitoylphosphatidylcholine, distearoylphosphatidylglycerol, and cholesterol were dissolved in a chloroform and methanol mixture and allowed to form a thin film within a rotatory evaporator. This thin film was hydrated with a sodium selenite (5.8 μM) solution to form multilamellar vesicles and homogenized under high pressure to yield unilamellar nanoliposomes. Se-loaded nanoliposomes were mannosylated by 0.1% *w/v* mannosamine (Man-Lip-Se) prior to being lyophilized. Mannosamine concentration was optimized with cellular uptake studies in M receptor expressing cells. Non-lyophilized and lyophilized Man-Lip-Se were characterized for size, zeta potential, and entrapment efficiency. The influence of liposomal composition on the characteristics of Man-Lip-Se were evaluated using acidic and basic medium for 24 h. Thermal analysis and powder X-ray diffraction were used to determine the interaction of components within the Man-Lip-Se. The size, zeta potential and entrapment efficiency of the optimum Man-Lip-Se were observed to be 158±28.9 nm, 33.21±0.89 mV, and 77.27±2.34%, respectively. An *in vitro* Se release of 70–75% up to 24 h in PBS pH 6.8 and <8% Se release in acidic media (0.1 N HCl) in 1 h was observed. The Man-Lip-Se were found to withstand gastric-like environments and showed sustained release. Stable freeze-dried Man-Lip-Se were successfully formulated with a size of <200 nm, ~75% entrapment, and achieved controlled release of Se with stability under acidic media, which may be of importance in the targeted delivery of Se to the immune system.

KEY WORDS: mannosylation; nanoliposome; selenium; thermal properties.

INTRODUCTION

Selenium (Se) is an essential nutritional trace element that impacts various aspects of human health (1–4). A number of epidemiological studies have reported that asthma incidence, prevalence, and/or severity are associated with reduced Se status (5–14). However, some of the studies were not able to establish the role of selenium (15,16). Nonetheless, epidemiological studies suggest that Se has beneficial immunomodulatory properties and Se supplementation may reduce allergic asthma (17–21). In our previous studies, oral Se supplementation was found to change immune responses from Th2-type to Th1/T_{reg}-types, which modulates levels of asthma in mice (22,23). Se administration increased glutathione peroxidase in lung tissue and inhibited the generation of hydrogen peroxide and the activation of nuclear factor kappa-light-chain-enhancer of activated B cells (NF-κB) induced by tumor necrosis factor-alpha (TNF-α), which may represent a major anti-inflammatory mechanism by which Se attenuates asthma (24).

Current Se supplementation approaches are not consistently effective at lowering allergic asthma in humans (25–27). In addition, there is emerging concern with off-target or adverse effects of long-term oral Se supplementation that includes possible increased risk of type-2 diabetes (28,29). Therefore, there is an unmet need to develop new supplementation approaches that selectively deliver Se to the immune system and thereby minimize the risk associated with whole body supplementation. Nanocarriers (NCs) have emerged as a viable delivery method for site-specific delivery of therapeutic agents. In a past study, Se nanoparticles prepared by adding bovine serum albumin to the redox reaction system of selenite and glutathione, showed a lower toxicity than Se compounds used in dietary supplementation but retained a similar ability to upregulate selenoenzymes (30,31). However, these Se nanoparticles have similar bioavailability compared to that of conventional Se supplementation and consequently they do not overcome the associated adverse side effects. Therefore, there is unmet need to develop targeted formulations which will specifically

Electronic supplementary material The online version of this article (doi:10.1208/s12249-013-9988-3) contains supplementary material, which is available to authorized users.

[1] Department of Pharmaceutical Science, College of Pharmacy, University of Hawai'i at Hilo, 34 Rainbow Drive, Hilo, Hawaii 96720, USA.
[2] Department of Cell and Molecular Biology, John A. Burns School of Medicine, University of Hawai'i, 651 Ilalo St, Honolulu, Hawaii, USA.
[3] To whom correspondence should be addressed. (e–mail: mahavir@hawaii.edu

deliver Se to the immune system while sparing normal tissues (31). NCs that preferentially shunt cargo to the immune system would allow low dosages of Se while avoiding the harmful side effects associated with conventional whole body Se supplementation approaches.

Intestinal lymphatic regions have been routinely explored for site-specific lymphatic delivery of orally administered proteins, drugs, and vaccines (32,33). The co-administration of lipid vehicle-based NCs enhanced the stimulation of chylomicron formation by enterocytes, which dissolve and assimilate lipophilic molecules into their nonpolar core and thus promote drug absorption into intestinal lymphatics (34). Furthermore, the mannose receptors present on the M cells overlying Peyer's patches represent an excellent target for specific delivery (33,35,36). Mannosamine interacts with mannose receptors present on M cells and has the added advantage of being mucoadhesive, which further promotes uptake by cells expressing the mannose receptor (37).

Liposomes consist of one or more lipid bilayers, encasing a hydrophilic core that contains the therapeutic agent and are usually sized within the nanoparticle level (38,39). Liposomes are versatile carriers due to their ability to function in aqueous solutions and they can be modified to add moieties for targeting uptake by particular cell-types. Liposomes are the most studied colloidal particle applied in medicine due to their biocompatibility and biodegradability. The targeting of M cells overlying Peyer's patches using NCs represents a promising delivery option. The delivery of therapeutic agents to M cells may be enhanced by using surface agents such as lectins, microbial adhesion molecules, and immunoglobulins that can bind to M cell surfaces selectively (33). Therefore, we have selected a mucoadhesive mannosamine to target the mannose receptors present on M cells to enhance the uptake of developed liposomes. In this investigation, we have focused on formulation and characterization of mannosamine-coated Se-loaded lipidic NCs (Man-Lip-Se). We hypothesized that the formulation of mannosamine-coated Se-loaded lipidic NCs (Man-Lip-Se) with critical parameters of particle size <200 nm, zeta potential >+10 mV, entrapment efficiency >60%, controlled release and that the mannosamine coating will increase the cellular uptake of cargo through M cell receptor-mediated endocytosis.

Therefore, the aims of this study were to formulate Se-loaded Man-Lip-Se and evaluate the effect of its composition on influencing parameters such as size, charge, entrapment efficiency and Se release at physiological relevant acidic and neutral media. The molecular characteristics of encapsulated Se within mannosylated nanoliposome using differential scanning calorimetry (DSC) and X-ray diffraction (XRD) techniques was also evaluated and reported herein. In addition, we have evaluated the cellular uptake of Man-Lip-Se using M receptor expressing MH-S macrophage cells. The deficiency of selenium in macrophage cells has been linked to asthma (40). For this investigation, we have used sodium selenite as the dietary source of Se. To the best of our knowledge, till date, this is the only literature explaining the development and evaluation of freeze-dried targeted mannosylated nanoliposomal formulation of Se.

MATERIALS AND METHODS

Materials

Dipalmitoyl phosphatidylcholine (DPPC) and distearoyl phosphatidyl glycerol (DSPG) were received as gift samples from Lipoid, Ludwigshafen, Germany. Sodium selenite, cholesterol (Chol), D-mannosamine HCl, ethylenediamine tetraacetic acid (EDTA), 2,3-diaminonapthalene (DAN), methanol, chloroform, dimethyl sulfoxide (DMSO), *O*-phthalaldehyde, potassium hydroxide, and boric acid were purchased from VWR International (Radnor, PA, USA). Spectra/Por Dialysis membrane (molecular weight cut off 25,000 Da) was obtained from Spectrum Laboratories Inc. (Rancho Dominguez, CA, USA). All chemicals used were of analytical grade. Deionized, 0.22 μm filtered sterile water was used throughout the experiments.

Preparation of Selenium-Loaded Nanoliposomes

Lip-Se were composed of DPPC, DSPG, and Chol and prepared using the thin film evaporation technique by using reported methods with slight variations (41–43). Lip-Se I, Lip-Se II, Man-Lip-Se I, and Man-Lip-Se II formulations were prepared as described in Fig. 1 and compositions are listed in Table I. These nanoliposome formulations were prepared in order to obtain a controlled release of Se and the mannosamine coating was optimized for cellular uptake. Briefly, DPPC (44 mg), DSPG (15.64 mg), Chol (14 or 17 mg) were dissolved in a mixture of chloroform/methanol (3:1) in 250 mL round-bottomed flask and subjected to dry thin formation in a Rotary evaporator (Heidolph, Schwabach, Germany) using a round-bottomed flask with rotation speed of 100 rpm for 4 h under 200±5 mmHg at a temperature of 55±2°C. The resultant thin film was hydrated with distilled water containing sodium selenite (1 mg/mL) with a rotary evaporator at 55±2°C for 45±1 min. The multilamellar vesicles formed were then passed through a high-pressure Nano DeBEE homogenizer (BEE International, South Easton, MA, USA) at 1000 psi for 1 cycle at 55°C. The HEPES buffer was added to this Lip-Se suspension and then centrifugation was performed using Vivaspin 500 centrifuge tubes with a filter of molecular cutoff weight of 10,000 Da (Viva Products, Inc., Littleton, MA, USA) at 16,200×*g* for 20 min and the Lip-Se pellet was collected for further preparation of Man-Lip-Se. The entrapped and unentrapped Se was determined by spectrophotometric analysis using Lip-Se pellets and the aqueous phase collected at the bottom of Vivaspin filter membrane respectively (44).

Preparation of Mannosamine-Coated Nanoliposomes

The mannosamine concentration of 0.1% *w*/*v* was selected to coat on the surface of nanoliposome based on maximum uptake of nanoliposomal in M receptor positive MH-S mouse alveolar cells as described below. The Lip-Se suspension (as described above) was incubated with 30 ml (0.1% *w*/*v*) mannosamine for 1 h at 25°C to form Man-Lip-Se. After incubation, the liposomes were centrifuged with HEPES buffer using Vivaspin ultracentrifuge tubes with filter membranes with molecular cut off weight of 10,000 Da (Viva Products, Inc., Littleton, MA, USA) at 16,200×*g* for 30 min and the Man-Lip-Se pellet and aqueous filtrate was collected for further

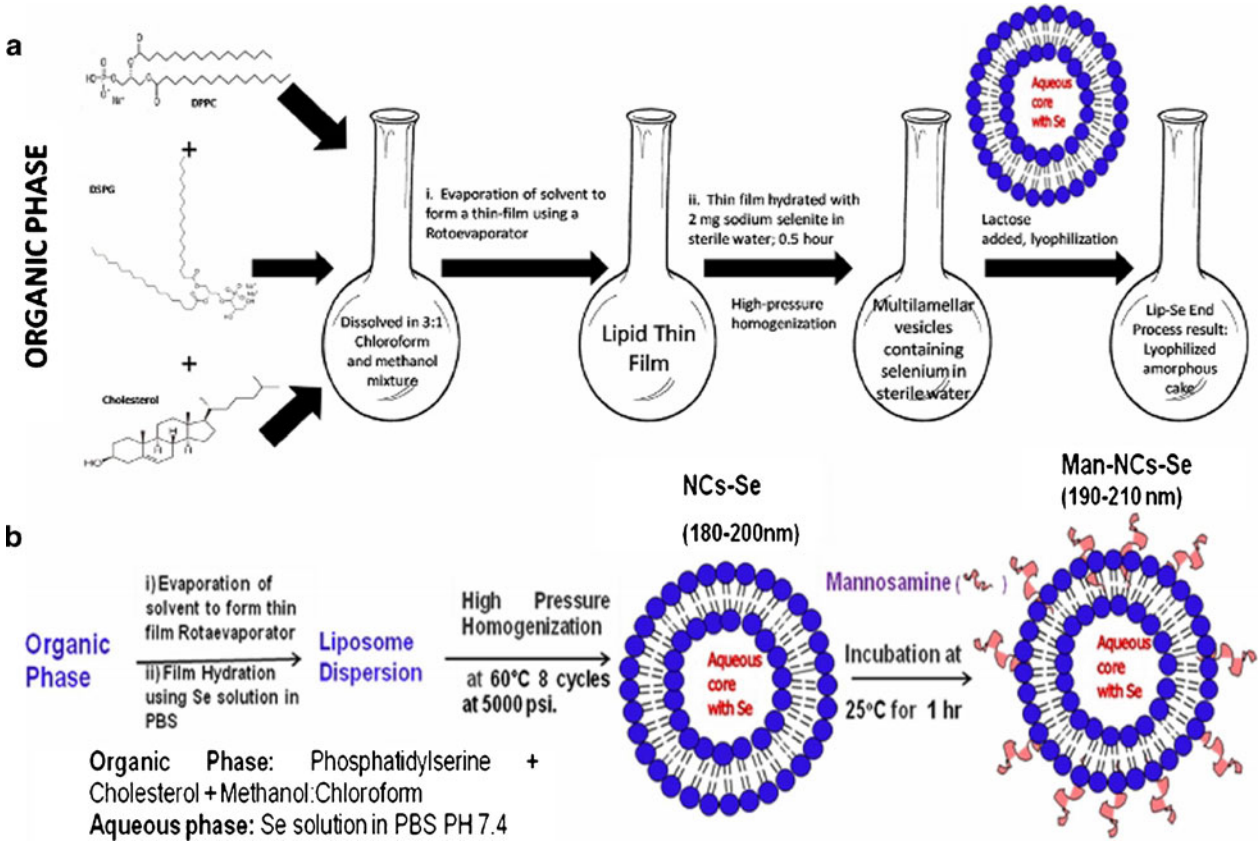

Fig. 1. Preparation procedure for Lip-Se liposomes. The DPPC, DSPG and Chol were dissolved in a chloroform and methanol mixture and allowed to form a thin film by rotoevaporation. The thin film was hydrated with distilled water containing 2 mg sodium selenite for 0.5 h to form multilamelllar vesicles followed by high-pressure homogenization. The Lip-Se suspensions were lyophilized using lactose monohydrate as a cryoprotectant

evaluation. The aqueous filtrate was quantified for unbound mannosamine using *O*-phthalaldehyde fluorimetric assay as described previously (45,46). The 1% *w/v* lactose monohydrate was used as a cryoprotectant and frozen to −80°C for 3 h. The frozen Man-Lip-Se suspension was lyophilized for 48 h under vacuum at <0.133 mbar at −84°C using Freeze one 12 Plus Lyophilizer (Labconco, Kansas City, MO, USA). The nanoliposome formulation suspension was prepared by resuspending the lyophilized formulation in deionized water for *in vitro* characterization. The formulation will be administered as a suspension *via* the oral route of administration. In our ongoing asthma mouse model studies, we will use the nanoliposome suspension formulation administered *via* oral route by gavage.

Particle Size and Zeta Potential Measurement

The particle size of the prepared nanoliposome was determined by dynamic light scattering using a NICOMP ZLS

Table I. Composition of Prepared Lip-Se I and II Liposomes. Man-Lip-Se I and II were Prepared with the Same Corresponding Lip-Se I and II Formulations, but with the Inclusion of the Addition of the Mannosamine Conjugation Step that is described in the "MATERIALS AND METHODS" Section

		Man-Lip-Se I	Man-Lip-Se II
Lipids	DPPC (mg)	44	44
	Chol (mg)	14	17
	DSPG (mg)	15.6	15.6
Organic Solvent	Chloroform (ml)	6	6
Mixture	MeOH (ml)	2	2
Hydration medium	1 M NaSe (μl)	11.6	11.6
	DI H_2O (ml)	qs 6	qs 6
Additional preparation methods		Homogenization, Lip-Se I was conjugated with mannosamine to form Man-Lip-Se I, Lyophilization	Homogenization, Lip-Se II was conjugated with mannosamine to form Man-Lip-Se II, Lyophilization

380 analyzer (PSS-NICOMP, Santa Barbara, USA). The particle size and zeta potential of the nanoliposomes were assessed by dispersion in deionized sterile water. The zeta potential was calculated by Smoluchowski's equation from the electrophoretic mobility of the nanoliposomes at 25°C. All measurements were recorded in triplicate (n=3).

Determination of the Extent of Mannosamine Coating

After resultant Man-Lip-Se suspension was centrifuged using Vivaspin and the aqueous filtrate was collected for further analysis of mannosamine content as described above. The unbound mannosamine was quantified using the collected aqueous filtrate using the *O*-phthalaldehyde fluorimetric assay (36). Mannosamine concentrations ranging from 5 to 100 μg/mL in distilled water were prepared for the development of a calibration curve. Then, 50 μl of test samples and standards were added to 150 μl of *O*-phthalaldehyde reagent in a 96-microwell plate. Two minutes after sample preparation, absorbance was determined at 340 nm using a Synergy H1 Hybrid plate reader for UV spectrophotometric analysis (BioTek Instruments, Inc., Winooski, VT, USA).

Nile Red-Loaded Liposomal Uptake of M receptor Positive MH-S Mouse Alveolar Cells

Nile red (NR) fluorescent dye-loaded Lip (Lip-NR) and Man-Lip-NR (Man-Lip-NR) were prepared by incorporating NR in the hydration medium and adding the solution to the thin film following similar methods used in the preparation of Man-Lip-Se. Various concentrations of mannosamine (0.05, 0.1, 0.3% *w*/*v*) were used to formulate the Man-Lip-NR. The MH-S cells were plated at 2,000 cells/well in a 96-well plate. The macrophages were incubated with 100 μL Lip-NR, Man-Lip-NR, Man-Lip-Se (negative control), and with NR solution dispersed in PBS and serum-free RPMI 1640 medium supplemented with 0.05 mM β-mercaptoethanol. The NR solution dispersed in serum-free RPMI medium and the Man-Lip-Se without NR were used as the positive and negative controls, respectively. At each image capture at 0.5, 15, 30, 60 min, the liposomal suspension and medium were removed and preserved in a sterile 96-well plate and the cells were washed with sterile DPBS to remove any traces of free NR. The cellular uptake of the Man-Lip-NR in mouse alveolar MH-S macrophages was investigated with fluorescence microscopy using a Zeiss Axiovert 40CFL microscope (Carl Zeiss Microscopy, LLC, USA). The fluorescent light source was an Exfo X-Cite series 120 (Lumen Dynamics Group, Inc., Mississauga, Ontario, Canada).

Se Analysis Assay

UV spectrophotometry was used for the analysis of Se, in a process where Se(VI) reacted with DAN to form a fluorescent Se-DAN heterocyclic compound as described previously (47,48). The addition of 2 mL 0.05 M EDTA and 2 mL 0.1% DAN to the Se solution facilitated the formation of piazselenol. The tube was incubated at 70°C for 30 min and then the piazselenol was extracted with 4 mL cyclohexane. The absorbance in the cyclohexane layer was measured at a wavelength of 378 nm using a Synergy H1 Hybrid plate reader for UV spectrophotometric analysis (BioTek Instruments, Inc., Winooski, VT, USA). The data was analyzed with Gen5™ 2.0 Data Analysis Software (BioTek Instruments, Inc., Winooski, VT, USA). The calibration curve of Se was prepared during each assay in standards with concentrations from 0 to 10 μg/mL. The correlation coefficient was consistently more than 0.99, and a detection limit of quantification was 0.5 μg/mL.

Determination of Entrapment Efficiency

For Se assay, 0.1 mL of the Lip-Se or Man-Lip-Se was dissolved in 0.2 mL each of methanol and DMSO (1:1) and subsequent dilutions were made with double distilled water. Prior to UV analysis, samples were centrifuged at 16,200×*g* for 10 min and the supernatant was analyzed for Se content. Entrapment efficiency was determined using Vivaspin500 ultracentrifuge filters with molecular cut off weight of 10,000 Da (Viva Products, Inc., Littleton, MA, USA). Briefly, the Lip-Se or Man-Lip-Se (0.1 mL) formulation was placed on top of the Vivaspin filter membrane (molecular weight cutoff 10,000 Da) and centrifuged at 16,200×*g* for 10 min. The aqueous filtrate was diluted appropriately and subjected to UV spectrophotometric analysis to determine the Se content. The entrapment efficiency (EE) of the Se within developed formulations were defined as the drug content that was entrapped into nanoliposomes, and calculated by using following equation.

$$\mathrm{EE}(\%) = \frac{\text{Total drug} - \text{Free selenite amount}}{\text{Total drug}} \times 100 \qquad (1)$$

In vitro Release of Se from Man-Lip-Se

In vitro release study of Se from various Man-Lip-Se was carried out in phosphate buffer saline (PBS) pH 6.8 and 0.1 N HCl solution pH 3.0 to simulate intestinal and gastric conditions, respectively. In addition, the *in vitro* release of Se from Man-Lip-Se II was also conducted in 0.1 N HCl for 2 h and then the medium was changed to PBS pH 6.8 to simulate gastric and intestinal conditions *in vivo*. Lyophilized Man-Lip-Se were re-suspended in PBS solution and placed in a dialysis membrane bag with molecular weight cutoff of 10,000 Da. The membrane bags were placed in 50 ml of PBS pH 6.8 or 0.1 N HCl solution pH 3.0 medium to simulate sink conditions. The entire system was maintained at 37°C with continuous stirring at approximately 300 rpm. At specific time intervals (0.5, 1, 2, 3, 4, 5, 6, 7, 24 h), 0.5 mL of dissolution medium was collected and 0.5 mL of fresh respective dissolution medium was replaced. For the simulation of gastric and intestinal pH during the release studies, membrane bags containing nanoliposomes were placed in 50 ml of 0.1 HCl and samples were taken as described above at time points of 0, 0.5, 1, and 2 h. Then the membrane bags containing nanoliposomes were transferred to 50 mL of PBS pH 6.8 and samples were taken as described above at the time points of 3, 4, 5, 6, 7, and 24 h. The samples were analyzed at each time interval using the established UV spectrophotometric method and the time *versus* percent Se release was plotted to evaluate the release profile of developed formulations (Fig. 2).

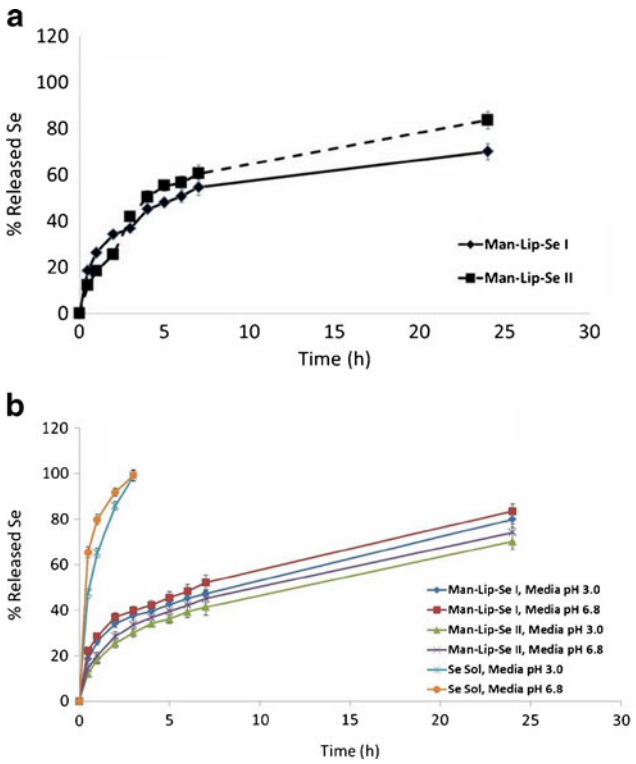

Fig. 2. **a** *In vitro* release data for the Man-Lip-Se formulation I and II in media of pH 3.0 for 0–2 h and pH 6.8 for 2–24 h. **b** *In vitro* release data for the Man-Lip-Se formulations I and II and selenium solution in media of pH 3.0 and pH 6.8

Molecular Interaction Evaluation using Differential Scanning Calorimetry

The interaction of Se with lipids and the association of Se within the Man-Lip-Se were evaluated using a DSC (DSC1, METTLER TOLEDO, Columbus, OH, USA). Approximately 2 mg of the Man-Lip-Se, unprocessed physical mixture of excipients and sodium selenite, individual excipient or sodium selenite alone were weighed into an aluminum pan and hermetically sealed, and the thermal behavior was determined in the range of −60°C to 225°C at a heating rate of 10°C min^{-1}. Baselines were determined using an empty pan, and all the thermograms were corrected for baseline. Transition temperatures were determined from the endothermic peak minima while transition enthalpies were obtained by integration of the endothermic transitions using linear baselines.

Molecular Interaction Evaluation using X-ray Diffraction Analysis

X-ray diffraction measurements of sodium selenite, lyophilized physical mixture of formulation constituents, lyophilized placebo Man-Lip (P-Man-Lip), and lyophilized Man-Lip-Se II were carried out with a powder XRD instrument, a Bruker D8 Advance (AXS GmbH, Karlsruhe, Germany) in the diffraction range of 5–40°. The PXRD diffraction instrument was equipped with a vertical goniometer in a Bragg–Brentano geometry ($\theta/2\theta$). The signal was conditioned using a Gobel mirror and collected using a LYNXEYE linear detector. A Cu-Kα radiation source was used, and the scanning (2θ) rate was 5°/min. Approximately 0.25 g of powder sample was filled into a glass sample holder and gently pressed down by a glass slide to make the sample surface and holder surface coplanar. The X-ray powder diffraction patterns of various formulations were analyzed for crystalline or amorphous characteristics.

Statistical Analysis

The experiments were conducted in triplicate with data reported as mean±standard deviation. Experimental statistics were performed using Minitab 16 Statistical Software (State College, PA, USA). A one-way analysis of variance (ANOVA) with Tukey's multiple comparison post-test was used in the analysis of differences between the physicochemical properties of nanoparticles with and without mannosamine conjugation. The least significant difference post-hoc ANOVA analysis was used in the comparison of particle sizes between Lip-Se and Man-Lip-Se formulations. The significance level was set at $p<0.05$.

RESULTS AND DISCUSSION

Asthma is a chronic disease in the USA and despite continued advances in asthma therapies, the clinical outcome remains poor (49). The immunomodulatory properties and effective therapeutic potential of Se for the treatment of asthma has drawn attention of researchers in recent years (2,50,51). However, available dietary Se supplements mainly consist of two inorganic forms, sodium selenate and sodium selenite, and one organic form, selenomethionine. Moreover, many studies reported that 50–90% of consumed selenite was lost and excreted in urine due to the short retention time in the gastrointestinal tract (52–54). It has been also evidenced that high dose supplementation of selenite may cause various adverse effects due to its pro-oxidant property, which depends on the concentration and other factors (55). Additionally, there is an emerging concern with potential adverse side effects of long-term oral Se supplementation methods that includes possible increased risk of type-2 diabetes (29). Therefore, providing efficient and safe application of dietary Se supplementation has become a challenging topic in recent years. Hence, we envisioned that the development of targeted Man-Lip-Se may prove as an efficacious and safe therapeutic modality compared to conventional long-term Se supplementation. Membranous epithelial cells termed micro fold cells (M cells) within the gastrointestinal tract are located within Peyer's patches (56–59). The M cells have a high transcytotic capacity and are capable of particulate transport of a number of materials directly to lymphoid follicles (60). A method of enhancing particle absorption within M cells is to attach mannosamine to the surface of the particles so that they can interact specifically with mannose receptor *via* receptor-mediated endocytotic mechanisms on the M cell apical membranes (33,61,62). Development of the nano-delivery system of Se compounds may improve delivery of Se directly to immune system to achieve desired effect using lower doses thereby limiting toxicities to normal tissues.

Unilammellar liposomes contain lipid bilayers that are able to encapsulate both hydrophobic and hydrophilic

therapeutic agents (63). Liposomes have the ability to transport therapeutic agents and dietary supplements through oral administration (64). The liposome preparation method should be chosen with the following parameters in mind: the physicochemical characteristics of the therapeutic agent, the characteristics of the dispersant medium, the concentration of the therapeutic agent, additional processes involved in the delivery of the liposomes, size, polydispersity and stability, and batch-to-batch reproducibility (65–67). Nanoliposomes are formed when sufficient energy is put into a system by forming the phospholipid bilayers (68). The use of sonication method has been limited due to lower entrapment efficiency or degradation of therapeutic agent (69,70). Similarly, we have also observed lower entrapment efficiency with the sonication method [data not shown]. The Mozafari method and the extrusion method of liposome preparation require specialized equipment and form larger sized liposomes respectively (71). We have selected a simple reproducible thin film hydration method to form multilamellar vesicles that were passed through high-pressure homogenizer to form unimellar nanoliposomes.

We have selected DPPC and DSPG, which are saturated phospholipids, to develop the Se-loaded nanoliposomal formulations owing to their stability advantages over unsaturated phospholipids (72,73). The Chol has been used to provide a sustained release profile and increase stability of the Man-Lip-Se (74,75). The nanoliposomes were formulated using thin film hydration technique as described within Fig. 1 and Table I.

The mean particle size ($n=3$) of various nanoliposomal formulations are shown in Table II. The Lip-Se I and II were found to be 148±68.7 and 154±23.0 nm, respectively. The mean particle size of Man-Lip-Se I and II were found to be 156±73.4 and 158±28.9 nm, respectively (Table II). The polydispersity index values of 0.36 and 0.05 were observed with Man-Lip-Se I and Man-Lip-Se II, respectively. The zeta potential of Lip-Se I and II were correspondingly −54.7±4.07 mV and −23.4±1.58 mV, respectively. The zeta potential of Man-Lip-Se I was 26.1±1.95 mV and Man-Lip-Se II was observed to be 33.2±0.89 mV. The lyophilized Man-Lip-Se II that had been reconstituted with sterile purified water were found to have a particle size of 159±62.4 nm and a zeta potential of 31.5±1.21 mV. The Man-Lip-Se II before and after lyophilization did not differ significantly ($p<0.05$) in particle size or zeta potential suggesting that the processing and storage methods, like lyophilization and storage at room temperature, are not detrimental to the physicochemical and biological properties of the Man-Lip-Se formulation (Table II).

Table II. Particle Size, Zeta Potential and Entrapment Efficiency Measurements for Lip-Se and Man-Lip-Se Formulations and Particle Size and Zeta Potential for Man-Lip-Se II after Lyophilization and Reconsitution

Nanoparticles	Particle size (nm)	Zeta Potential (mV)	EE initial
Lip-Se I	148±68.7	−54.7±4.07	73.3±2.49%
Lip-Se II	154±23.0	−23.4±1.58	74.0±3.57%
Man-Lip-Se I	156±73.4	26.1±1.95	73.3±2.49%
Man-Lip-Se II	158±28.9	33.2±0.89	77.3±2.34%
Reconstituted Man-Lip-Se II after lyophilization	159±62.4	31.5±1.21	99.5±2.46%[a]

[a] The represented data is for the Se assay since the unentrapped Se was removed before lyophilization

The fate of any drug delivery system after *in vivo* administration mainly depends on its physicochemical properties in relation to the body's physiological barriers (76–78). Physical parameters such as size and zeta potential affects stability, biodistribution, release pattern and cellular uptake of liposomes both *in vitro* and *in vivo* (79). The determination of encapsulation of Se within liposomes is also important for the stability, dose calculation and prediction of efficacy. As shown in Table II, the entrapment efficiency of Lip-Se I, Lip-Se II, Man-Lip-Se I and Man-Lip-Se II were found to be >70%. The entrapment efficiencies for Lip-Se I and Man-Lip-Se I were 73.0±2.49%, Lip-Se II and Man-Lip-Se II were 74.0±3.57% and 77.3±2.34%, respectively.

As shown in Table II, the mean sizes for Man-Lip-Se were higher compared to Lip-Se which suggests the increase in size due to the mannosamine coating. The increase of cholesterol from Lip-Se I to Lip-Se II and from Man-Lip-Se I to Man-Lip-Se II led to an increase in size, surface charge, and entrapment efficiency of these nanoliposomes. The observed positive shift of zeta potential Man-Lip-Se compared to Lip-Se is suggestive to successfully coating with mannosamine on the surface of developed nanoliposomes (Table II). The negative surface charge of the Lip-Se facilitates the conjugation of the protonated mannosamine at pH 7.0 by electrostatic attraction. The nature of high surface charge (+27 to 50 mV) in the Man-Lip-Se is likely to facilitate their absorption through the gastrointestinal tract, due to the molecular attractive forces formed by an electrostatic interaction between positively charge Man-Lip-Se and negatively charged mucosal surfaces and binding to M cells within Peyer's patches. The extent of coating of mannosamine on the surface of Man-Lip-Se (per milligram) was calculated using unbound mannosamine. The Man-Lip-Se was found to contain 20 μg of mannosamine/mg of nanoliposomes. It is shown in Table II that Se could considerably be entrapped into both Lip-Se and Man-Lip-Se, where the entrapment efficiency (% EE) of >70% as calculated using the Se assay standard curve equation $y=6.044x$ with an R^2 value equal to 0.992. Our results suggest that the developed formulation exhibited acceptable size, surface charge and entrapment efficiency. Similarly, Paliwal *et al.* reported that the liposome of soya lecithin prepared using thin film hydration technique were found to have a size and entrapment of 160.3±10.2 nm and 72.8±6.5%, respectively (80).

The results of the Man-Lip-NR uptake in M receptor positive MH-S mouse alveolar macrophages at 15 min post treatment are shown in Fig. 3. These results illustrate that the fluorescent NR uptake reaches a peak at a mannosamine concentration of 0.1% *w/v* and further increase in the mannosamine concentration of 0.3% *w/v* resulted in the saturation effect. Therefore, we have selected the mannosamine concentration of 0.1% *w/v* to formulate the Man-Lip-Se formulations (Fig. 3). Images were taken at the following time points 0, 5, 15, 30, and 60 min [see supplementary data Fig S1]. No morphological changes were observed in the macrophages during the 1 h incubation period.

After evaluating the physiochemical properties of nanoliposomes, *in vitro* release experiments were performed to test the release of Se from developed formulations using pH 3.0

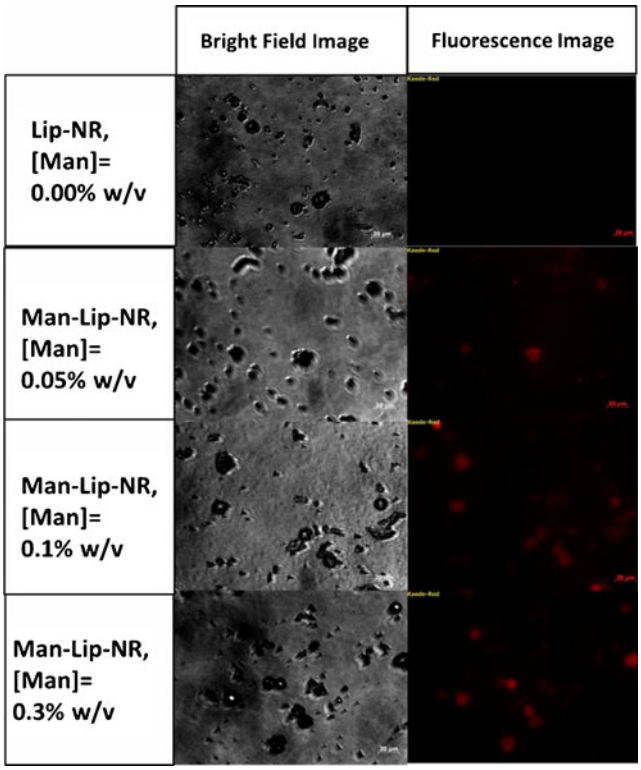

Fig. 3. Cell uptake of the Lip-NR and Man-Lip-NR at varying concentrations of mannosamine coating in M receptor positive mouse alveolar MH-S macrophages shown by fluorescence microscopy. Images were captured at a magnification of 40× using a three-position reflector slider P&C engaged in the red filter position. The *scale bars* are equal to 20 μm

and pH 6.8 media (Fig. 3). Liposomal dosage forms allow for the variation and retention control of drugs within physiological conditions (81–83). There are many causes of biological destabilization of liposomes to obtain a release of its contents. Temperature- and pH-sensitive liposomes are reliant on an environmental change that triggers the release of the therapeutic agent (84,85). The lipid bilayer of the liposome may fuse with the lipid bilayers of cell membranes to deliver their hydrophilic contents to the inside of a cell (86,87).

To simulate the intestinal and gastric environment after oral administration, *in vitro* release was studied at two different release media: PBS at pH 6.8 and 0.1 N HCl at pH 3.0. To study the release of the nanoliposomal suspension within a physiologically relevant medium, we have performed release within 0.1 N HCl at pH 3.0 for 2 h at which point the medium was changed to PBS at pH 6.8 for the later time points up to 24 h. The cumulative release of Se from Man-Lip-Se in pH 3.0 and pH 6.8 media to simulate the environment of the stomach and small intestine were compared (Fig. 3). *In vitro* release of Se from the Man-Lip-Se was evaluated using 50 mL of dissolution medium under sink conditions. As shown in Fig. 3a, the Man-Lip-Se I and II show an initial burst release for the first 0–2 h with 29.8±6.1% at 2 h in pH 3.0 medium and a slower sustained release between 2 and 24 h. As shown in Fig. 3b, Man-Lip-Se I showed an initial burst release for the first 0–3 h with 37.6±2.0% and 40±2.0% at 3 h in the pH 3.0 and pH 6.8 dissolution media, respectively. The Man-Lip-Se II showed a slower rate of Se release compared to Man-Lip-Se I in both pH 3.0 and pH 6.8 media. Man-Lip-Se I and Man-Lip-Se II showed >80% and >70% release at 24 h in both the pH 3.0 and pH 6.8 media, respectively. The increase in cholesterol between the Man-Lip-Se I and Man-Lip-Se II batches lead to a decrease in initial burst rate, followed by a slower prolonged release effect.

In contrast, the Se solution showed 100% release within 3 h in both pH 3.0 and pH 6.8 media. Our results showed that the release pattern of the Man-Lip-Se illustrated that there was no significant ($p<0.05$) differences in release behavior compared to that of Lip-Se [data not shown]. The percentage of Se release from developed nanoliposomes was relatively faster in the presence of PBS pH 6.8 dissolution media compared to the 0.1 N HCl pH 3.0 medium. Man-Lip-Se II showed delayed release at all time points due to the presence of higher concentration of cholesterol compared to Man-Lip-Se I (Fig. 3). In addition, we have observed that use of lower concentration of Chol within Man-Lip-Se I showed significant ($p<0.05$) initial burst release in both medium [data not shown]. Above all, it was important to prepare dispersion of freeze dried liposomes with water to form a liposomal suspension; otherwise, the freeze dried liposomes powders would stick to the dialysis bag, thus affecting drug release from the liposomal suspension. The report by Chu *et al.* showed that the dispersion of proliposomes is desirable compared to freeze dried proliposomes for release studies (42).

The addition of cholesterol to liposomes is known to affect the interaction of bilayers and bilayer stability. The crystallization of hydrocarbon chains of saturated lipids can be hindered by the use of Chol, leading to a gel state system (88). Virden and Birg found that the increase in Chol concentration in unilamellar DPPG based liposomes resulted in decreased aggregation (89). Chol within a liposomal formulation has the potential to influence the *in vitro* drug release properties. The amount of Chol within a liposomal formulation is inversely proportional to the *in vitro* release rates of encapsulated therapeutic agent (74). An optimized liposomal drug delivery system should be stable under physiological conditions, yet be permeable and capable of drug release to the target site of action. Similar to our results, the incorporation of cholesterol with a liposomal formulation produced retardation in the release of doxorubicin and arabinofuranosyl cytidine (ara-C), whereas, at a higher mole percent, a much larger release rate of idarubicin was observed compared to cholesterol-free liposomes (90–92). A study by Taira *et al.* showed that liposomes composed of egg phosphatidylcholine and cholesterol were found to be most stable within acidic gastric simulated media (pH 2) (93).

The observed sustained release of Se for 24 h from Man-Lip-Se in the pH 3.0 and pH 6.8 medium suggests that the nanoliposomes are stable at physiological pH, thus presenting the feasibility of the developed nanoliposomes for the delivery to the immune system. We have selected the Man-Lip-Se II for further evaluation based on Se release <20% at 1 h in the pH 3.0 and pH 6.8 media.

Differential scanning calorimetric thermal analysis can be utilized to study the interactions between the molecules forming the nanoliposome and may determine the incorporation of drugs within nanoparticles through the examination of enthalpy changes (44,94,95). DSC is a thermoanalysis method for measuring the temperature and heat flow associated with

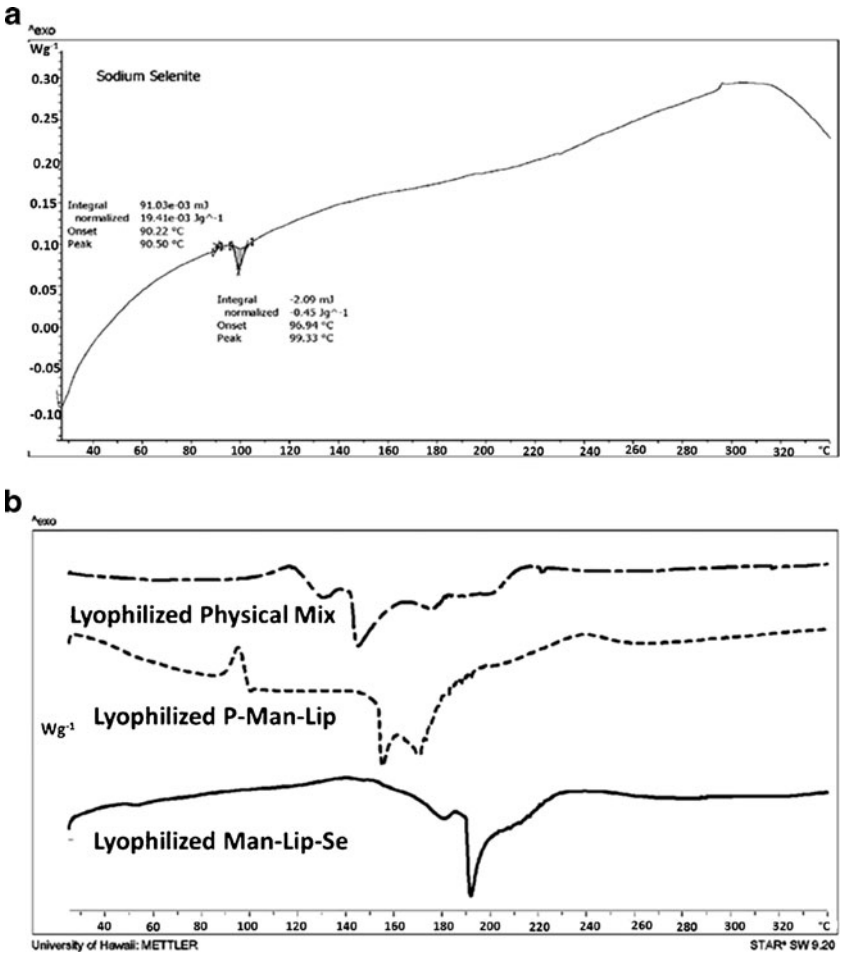

Fig. 4. DSC thermograms for lyophilized sodium selenite (**a**) and lyophilized physical mixture of formulation constituents, lyophilized P-Man-Lip, and lyophilized Man-Lip-Se (**b**)

transitions in materials as a function of time. Results from DSC can provide information on the endothermic or exothermic phenomena that occurs due to physical and chemical changes or changes in heat capacity (96). For lipid dispersions, such as liposomes, DSC is a method of characterization of the matrix state, consisting of polymorphism and drug entrapment and component interactions. Nanoliposomes have DSC characteristics that are unique from bulk materials, such as: decreased melting points, different melting points and enthalpies based on lipid polymorphism, and endotherm broadening due to multiple lipid components and size differences (97).

After evaluating the release behavior of the developed formulations, we have evaluated the thermal and powder diffraction characteristics using DSC and XRD. DSC was carried on lyophilized samples of physical mixture of excipients, P-Man-Lip, and Man-Lip-Se II to evaluate the interaction of Se with lipids in physical mixture and nanoliposome formulation and the entrapment of Se inside the nanoliposomes in molecular dispersion form. The results of DSC studies are represented in Fig. 4. The thermogram of sodium selenite (Fig. 4) showed a broad endotherm at 99.33°C, whereas physical mixture form of the sodium selenite showed a shorter endotherm shifted to approximately 130°C and another endotherm at approximately 145°C due to additives within the physical mixture. Interestingly, the thermogram for the Man-Lip-Se II showed an absence of corresponding endotherm for sodium selenite at 99.33°C or 130°C (Fig. 4). The thermograms for the Man-Lip-Se II show an endotherm peaks at approximately 190°C. The individual excipients were also analyzed by DSC [see supplementary data Fig S2A–H]. The following melting point onsets and peaks were obtained for the individual excipients: Lactose monohydrate had a melting onset temperature of 211.92°C and peak of 217.33°C, Cholesterol had a melting onset of 136.03°C and peak of 140.83°C, DPPC had a melting onset of 60.55°C and peak 63.50°C, D-mannosamine hydrochloride had a melting onset temperature of 167.09°C and peak of 173.17°C.

The data illustrate that the Man-Lip-Se composed of DPPC, DSPG and Chol resulted in the broadening of the endothermic peak compared to the individual lipid component thermograms alone (Figs. 4 and 5, supplementary data). Similar findings were found in a study by Aburahma and Abdelbary where DSC was performed on a physical mixture of lipids, individual components, and proliposomes (98). The thermogram of Man-Lip-Se displayed slight narrowing and shifting of the melting endotherm due to the unique molecular interaction within the nanoliposomes. These results demonstrated that the Man-Lip-Se were not a physical mixture of their untreated components which is suggestive of encapsulation of Se within nanoliposomes.

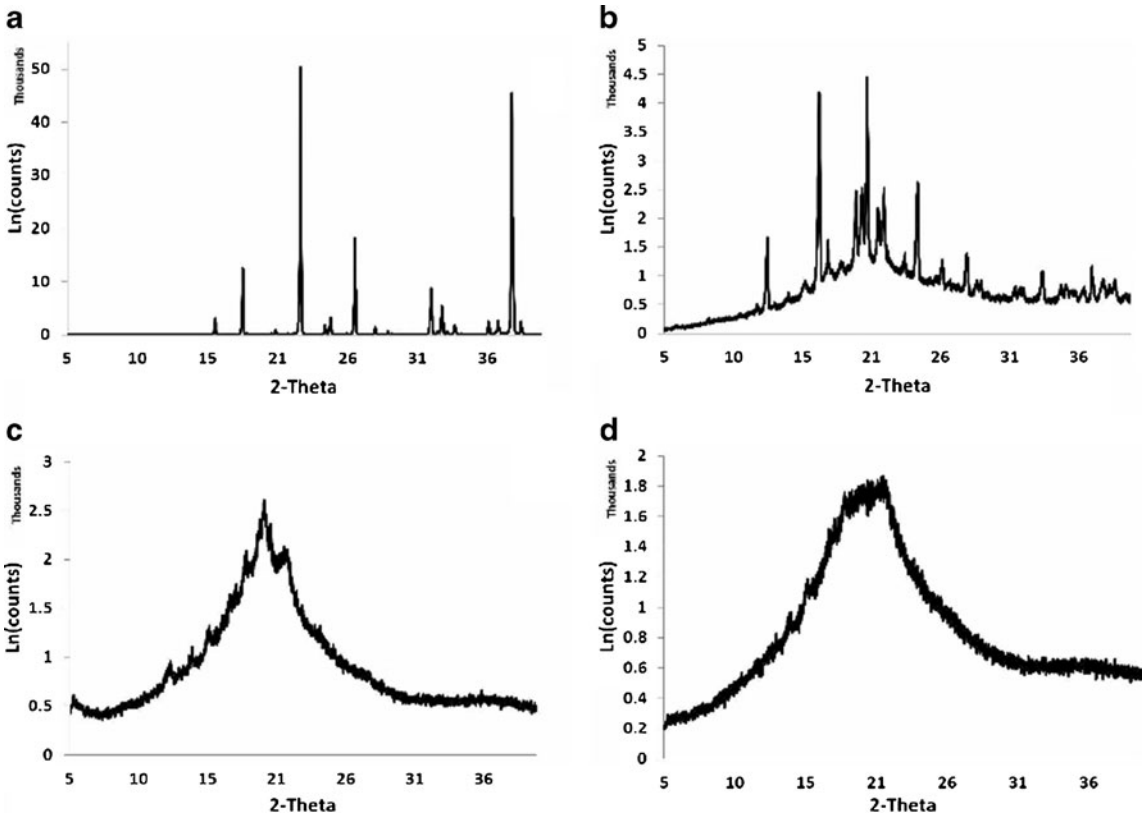

Fig. 5. Powder XRD patterns of sodium selenite (**a**), the lyophilized physical mixture of formulation constituents (**b**), lyophilized placebo liposomes (**c**), and Man-Lip-Se (**d**). Crystallinity can be seen with the lyophilized sodium selenite and the physical mixture, whereas the lyophilized placebo- and selenium-loaded formulated liposomes display amorphous characteristics. Type: 2Th/Th locked; Start: 5.000°–End: 39.996°; Step: 0.010°; Step time: 96 s; Temp: 25°C (Room); Time started: 4 s; 2-Theta: 5.000°–Theta: 2.500°

To investigate the crystalline or amorphous state of encapsulated Se within nanoliposomes, we studied diffraction pattern of sodium selenite, the lyophilized physical mixture of formulation constituents, lyophilized blank liposomes, and the lyophilized Man-Lip-Se (Fig. 5). The crystalline or amorphous state of drug encapsulated in the nanoparticles needs to be evaluated in order to ascertain the level and quality of sodium selenite encapsulation within the hydrophilic core of the unilamellar nanoliposome. The diffraction patterns of individual samples of sodium selenite, lyophilized physical component mixture, lyophilized P-Man-Lip, and lyophilized Man-Lip-Se II are shown in Fig. 5. The sodium selenite (Fig. 5a) and the lyophilized physical mixture (Fig. 5b) of formulation components showed more crystallinity, whereas the lyophilized P-Man-Lip and Man-Lip-Se II displayed amorphous properties (Fig. 5c–d).

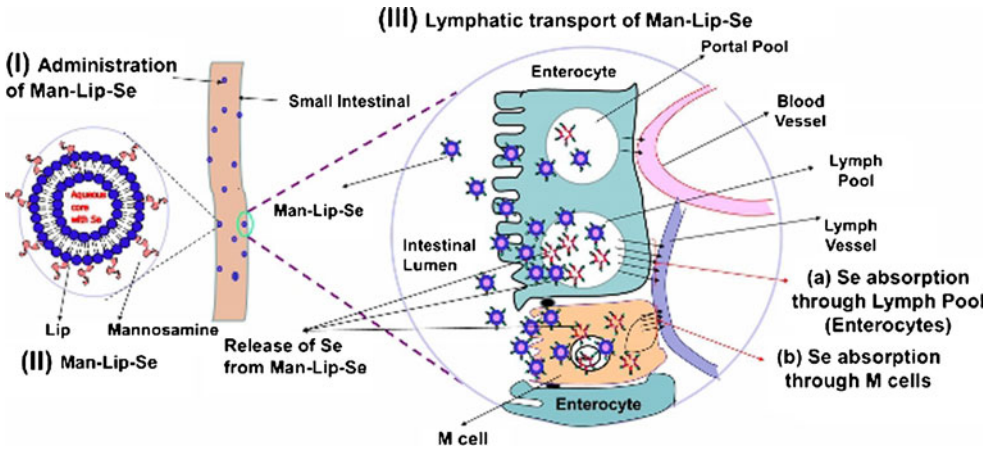

Fig. 6. Targeted Delivery of Se to the Immune System. (*I*) Administration of Man-Lip-Se; (*II*) design of Man-Lip-Se; and (*III*) Se delivery to immune system using Man-Lip-Se; (*a*) Absorption of Se through the lymph pool due to lipidic NCs; and (*b*) selective interaction of Man-Lip-Se with mannose receptors present on the M cells resulting in efficient Se transport to immune system

The diffraction pattern of sodium selenite (Fig. 5a) showed remarkable difference from those of Man-Lip-Se II (Fig. 5d). The sharp peaks of Se indicating the crystalline nature were not present in the diffraction pattern of Man-Lip-Se II indicating that encapsulated Se is amorphous or molecular dispersion form. Also, there was a small difference in the diffraction patterns of the placebo Man-Lip (P-Man-Lip), and Man-Lip-Se II, indicating that the encapsulated of Se and/or coating of Man has not changed the nature of liposomes. XRD patterns of the P-Man-Lip and Man-Lip-Se II were broader and much weaker than that of the physical mixture indicating the less ordered or loosely arranged structure of nanoliposomes. As Hancock and Zografi reported, the crystalline to amorphous transition of a solid state form is advantageous for dissolution enhancement because an amorphous drug material does not require the energy to overcome the crystalline lattice (99).

Lectin surface-modified particulates have the opportunity to specifically interact with the apical membrane of M cells (100,101). Mannosamine is a positively charged mucoadhesive and found to enhance uptake through M cells within Peyer's patches due to interaction with mannose receptors expressed on the gut mucosa and lymphoid tissue (62,102). M cells have a high transcytotic capacity, making them able to transport many materials and particulates. Therefore, they are a potential gateway for the delivery of drugs, vaccines, and other biologics (33,103,104). The coating of mannosamine on the surface of the Se-loaded nanoliposomes will serve as mucoadhesive and ligand for mannose receptor loaded on M cells. We have established a murine model of asthma in our laboratory to evaluate the efficacy of anti-asthmatic therapies (23). Our ongoing studies are focused to investigate the evaluation of pharmacokinetic parameters in Balb/c mice and testing of Man-Lip-Se on an asthma animal model to confirm the enhanced *in vivo* efficacy of prepared targeted formulation of Se compared to an orally administered Lip-Se and Se solution. Our previous studies found that the Se dose of 4 μg of Se/day was found to be effective in alleviating asthma (23,105). We plan to use Se equivalent oral dose of 2 and 4 μg administered twice per week to evaluate the anti-asthmatic efficacy of nanoliposomes and conventional supplement for our future mouse model studies. We outlined our proposed targeted delivery approach to the immune system in Fig. 6. The mannosylated nanoliposomal formulation developed by us will help to enhance the lymphatic absorption of Se *via* M cell targeted mucoadhesive lipid nanoliposomes to exert the desired effects. This novel use of nanoliposomal delivery of Se may provide a means by which Se may be selectively delivered to the target site. This approach may also help to reduce the required dose of Selenium, thereby reducing the associated adverse side effects to normal tissues.

CONCLUSION

Mannosylated Se-loaded nanoliposomes comprising of DSPG, DPPC, and Chol were successfully prepared using thin film hydration technique. The particle size, zeta potential, and entrapment efficiency of the optimum Man-Lip-Se was 158± 2.89 nm, 33.21±0.89 mV, and 77.27±2.34%, respectively. The size, zeta potential, and mannosamine assay suggested the successfully coating of mannosamine on the surface of Se-loaded nanoliposomes. The M receptor uptake studies performed utilizing MH-S mouse alveolar macrophages revealed that a mannosamine concentration of 0.1% *w/v* reached a saturation effect. The Man-Lip-Se was able to release the Se in a controlled manner for a prolonged period of time in the physiologically relevant dissolution medium. DSC and XRD studies demonstrated a clear difference between the Man-Lip-Se and the physical mixture, which is indicated the association encapsulated Se at molecular dispersion form within developed Man-Lip-Se. This investigation explored the formulation and evaluation of targeted mannosylated Se-loaded nanoliposomes with a vision of shunting Se to the immune system for enhanced anti-asthmatic effect and lowered adverse side effects.

ACKNOWLEDGEMENTS

We acknowledge the 2011 and 2013 Leahi Fund to Treat & Prevent Pulmonary Disease of the Hawai'i Community Foundation, Honolulu, HI, USA for research support on asthma and mesothelioma research, respectively to Dr. Mahavir B. Chougule. We would like to acknowledge the 2013 George F. Straub Trust and Robert C. Perry Fund of the Hawai'i Community Foundation, Honolulu, HI, USA for research support on lung cancer. We also acknowledge seed grant from the Research Corporation of the University of Hawai'i at Hilo, HI, USA and University of Hawaii at Hilo College of Pharmacy for providing start up financial support to our research group. We acknowledge the input of Dr. Rakesh Kumar Tekade, postdoctoral fellow, Dept. of Pharmaceutical Sciences, College of Pharmacy, University of Hawaii at Hilo, HI, USA.

REFERENCES

1. Navarro-Alarcon M, Lopez-Martinez MC. Essentiality of selenium in the human body: relationship with different diseases. Sci Total Environ. 2000;249(1–3):347–71. PubMed PMID: 10813463. Epub 2000/05/17. eng.
2. Huang Z, Rose AH, Hoffmann PR. The role of selenium in inflammation and immunity: from molecular mechanisms to therapeutic opportunities. Antioxid Redox Signal. 2012;16(7):705–43. PubMed PMID: 21955027. Pubmed Central PMCID: PMC3277928. Epub 2011/10/01. eng.
3. Fairweather-Tait SJ, Bao Y, Broadley MR, Collings R, Ford D, Hesketh JE, *et al*. Selenium in human health and disease. Antioxid Redox Signal. 2011;14(7):1337–83. PubMed PMID: 20812787. Epub 2010/09/04. eng.
4. Brinkman M, Buntinx F, Muls E, Zeegers MP. Use of selenium in chemoprevention of bladder cancer. Lancet Oncol. 2006;7:766–74.
5. Stone R. A medical mystery in middle China. Science. 2009;324(5933):1378–81. PubMed PMID: WOS:000266878700008.
6. Flatt A, Pearce N, Thomson CD, Sears MR, Robinson MF, Beasley R. Reduced selenium in asthmatic subjects in New Zealand. Thorax. 1990;45(2):95–9. PubMed PMID: 2315881. Pubmed Central PMCID: PMC462313. Epub 1990/02/01. eng.
7. Hasselmark L, Malmgren R, Unge G, Zetterstrom O. Lowered platelet glutathione-peroxidase activity in patients with intrinsic asthma. Allergy. 1990;45(7):523–7. PubMed PMID: WOS:A1990EC54200006.
8. Kocyigit A, Armutcu F, Gurel A, Ermis B. Alterations in plasma essential trace elements selenium, manganese, zinc, copper, and iron concentrations and the possible role of these elements on oxidative status in patients with childhood asthma. Biol Trace Elem Res. 2004;97(1):31–41. PubMed PMID: WOS:000188192800003.
9. de Luis DA, Izaola O, Aller R, Armentia A, Cuellar L. Antioxidant and fat intake in patients with polinic asthma. Medicina Clinica. 2003;121(17):653–4. PubMed PMID: WOS:000187618300004.

10. Qujeq D, Hidari B, Bijani K, Shirdel H. Glutathione peroxidase activity and serum selenium concentration in intrinsic asthmatic patients. Clin Chem Lab Med. 2003;41(2):200–2. PubMed PMID: WOS:000181095800014.
11. Omland O, Deguchi Y, Sigsgaard T, Hansen JC. Selenium serum and urine is associated to mild asthma and atopy. The SUS study. J Trace Elem Med Biol. 2002;16(2):123–7. PubMed PMID: WOS:000177406700009.
12. Misso NLA, Powers KA, Gillon RL, Stewart GA, Thompson PJ. Reduced platelet glutathione peroxidase activity and serum selenium concentration in atopic asthmatic patients. Clin Exp Allergy. 1996;26(7):838–47. PubMed PMID: WOS:A1996UY84300015.
13. Kadrabova J, Madaric A, Kovacikova Z, Podivinsky F, Ginter E, Gazdik F. Selenium status is decreased in patients with intrinsic asthma. Biol Trace Elem Res. 1996;52(3):241–8. PubMed PMID: WOS:A1996UV44000003.
14. Shaw R, Woodman K, Crane J, Moyes C, Kennedy J, Pearce N. Risk-factors for asthma symptoms in Kawerau children. New Zeal Med J. 1994;107(987):387–91. PubMed PMID: WOS:A1994PN14500001.
15. McKenzie RC, Rafferty TS, Beckett GJ. Selenium: an essential element for immune function. Immunol Today. 1998;19(8):342–5. PubMed PMID: WOS:000075213400002.
16. Ford ES, Mannino DM, Redd SC. Serum antioxidant concentrations among US adults with self-reported asthma. J Asthma. 2004;41(2):179–87. PubMed PMID: WOS:000220964200006.
17. Thomson CD, Wickens K, Miller J, Ingham T, Lampshire P, Epton MJ, *et al*. Selenium status and allergic disease in a cohort of New Zealand children. Clin Exp Allergy. 2012;42(4):560–7. PubMed PMID: 22417214. Epub 2012/03/16. eng.
18. Patelarou E, Giourgouli G, Lykeridou A, Vrioni E, Fotos N, Siamaga E, *et al*. Association between biomarker-quantified antioxidant status during pregnancy and infancy and allergic disease during early childhood: a systematic review. Nutr Rev. 2011;69(11):627–41. PubMed PMID: 22029830. Epub 2011/10/28. eng.
19. van Oeffelen AAM, Bekkers MBM, Smit HA, Kerkhof M, Koppelman GH, Haveman-Nies A, *et al*. Serum micronutrient concentrations and childhood asthma: the PIAMA birth cohort study. Pediatr Allergy Immunol. 2011;22(8):784–93. PubMed PMID: WOS:000298095300005.
20. Nurmatov U, Devereux G, Sheikh A. Nutrients and foods for the primary prevention of asthma and allergy: systematic review and meta-analysis. J Allergy Clin Immunol. United States: Asthma & Immunology. Published by Mosby; 2011;127:724–33 e1-30.
21. Bakkeheim E, Mowinckel P, Carlsen KH, Burney P, Carlsen KC. Altered oxidative state in schoolchildren with asthma and allergic rhinitis. Pediatr Allergy Immunol. 22. England: 2010 Wiley. 2011. 178–85.
22. Hoffmann PR, Saux CJL, Hoffmann FW, Chang PS, Bollt O, He QP, *et al*. A role for dietary selenium and selenoproteins in allergic airway inflammation. J Immunol. 2007;179(5):3258–67. PubMed PMID: WOS:000248991800068.
23. Hoffmann FW, Hashimoto AC, Shafer LA, Dow S, Berry MJ, Hoffmann PR. Dietary selenium modulates activation and differentiation of CD4(+) T cells in mice through a mechanism involving cellular free thiols. J Nutr. 2010;140(6):1155–61. PubMed PMID: WOS:000277800700015.
24. Jeong DW, Yoo MH, Kim TS, Kim JH, Kim IY. Protection of mice from allergen-induced asthma by selenite—prevention of eosinophil infiltration by inhibition of NF-kappa B activation. J Biol Chem. 2002;277(20):17871–6. PubMed PMID: WOS:000175685100062. English.
25. May SW. Selenium-based drug design: rationale and therapeutic potential. Expert Opin Investig Drugs. 1999;8(7):1017–30. PubMed PMID: 15992103. Epub 2005/07/05. eng.
26. Venardos KM, Perkins A, Headrick J, Kaye DM. Myocardial ischemia-reperfusion injury, antioxidant enzyme systems, and selenium: a review. Curr Med Chem. 2007;14(14):1539–49. PubMed PMID: 17584062. Epub 2007/06/23. eng.
27. Ferguson LR, Karunasinghe N. Nutrigenetics, nutrigenomics, and selenium. Front Genet. 2011;2:15. PubMed PMID: 22303312. Pubmed Central PMCID: PMC3268570. Epub 2012/02/04. eng.
28. Dunn BK, Richmond ES, Minasian LM, Ryan AM, Ford LG. A nutrient approach to prostate cancer prevention: the Selenium and Vitamin E Cancer Prevention Trial (SELECT). Nutr Canc Intl J. 2010;62(7):896–918. PubMed PMID: WOS:000282583200007.
29. Stranges S, Marshall JR, Natarajan R, Donahue RP, Trevisan M, Combs GF, *et al*. Effects of long-term selenium supplementation on the incidence of type 2 diabetes: a randomized trial. Ann Intern Med. 2007;147:217–23.
30. Wang D, Taylor EW, Wang Y, Wan X, Zhang J. Encapsulated nanoepigallocatechin-3-gallate and elemental selenium nanoparticles as paradigms for nanochemoprevention. Int J Nanomed. 2012;7:1711–21.
31. Zhang JS, Gao XY, Zhang LD, Bao YP. Biological effects of a nano red elemental selenium. Biofactors. 2001;15(1):27–38. PubMed PMID: 11673642. Epub 2001/10/24. eng.
32. Caliph SM, Charman WN, Porter CJH. Effect of short-, medium-, and long-chain fatty acid-based vehicles on the absolute oral bioavailability and intestinal lymphatic transport of halofantrine and assessment of mass balance in lymph-cannulated and non-cannulated rats. J Pharm Sci. 2000;89(8):1073–84. PubMed PMID: WOS:000088733500012.
33. Clark MA, Jepson MA, Hirst BH. Exploiting M cells for drug and vaccine delivery. Adv Drug Deliv Rev. 2001;50(1–2):81–106. PubMed PMID: WOS:000171145500006.
34. Porter CJH, Charman WN. Intestinal lymphatic drug transport: an update. Adv Drug Deliv Rev. 2001;50(1–2):61–80. PubMed PMID: WOS:000171145500005.
35. Salman HH, Irache JM, Gamazo C. Immunoadjuvant capacity of flagellin and mannosamine-coated poly(anhydride) nanoparticles in oral vaccination. Vaccine. 2009;27(35):4784–90. PubMed PMID: WOS:000268827500010.
36. Salman HH, Gamazo C, Campanero MA, Irache JM. Bioadhesive mannosylated nanoparticles for oral drug delivery. J Nanosci Nanotechnol. 2006;6(9–10):3203–9. PubMed PMID: WOS:000240865900070.
37. Kaur CD, Nahar M, Jain NK. Lymphatic targeting of zidovudine using surface-engineered liposomes. J Drug Target. 2008;16(10):798–805. PubMed PMID: WOS:000260851900008.
38. Lian T, Ho RJ. Trends and developments in liposome drug delivery systems. J Pharm Sci. 90. United States: 2001 Wiley-Liss; 2001. p. 667–80.
39. Szelenyi I. Nanomedicine: evolutionary and revolutionary developments in the treatment of certain inflammatory diseases. Inflamm Res. 2012;61(1):1–9. PubMed PMID: 22057873. Epub 2011/11/08. eng.
40. Vunta H, Belda BJ, Arner RJ, Channa Reddy C, Vanden Heuvel JP, Sandeep Prabhu K. Selenium attenuates pro-inflammatory gene expression in macrophages. Mol Nutr Food Res. 2008;52(11):1316–23. PubMed PMID: 18481333. Epub 2008/05/16. eng.
41. Chougule M, Padhi B, Misra A. Development of spray dried liposomal dry powder inhaler of Dapsone. AAPS PharmSciTech. 2008;9(1):47–53. PubMed PMID: 18446460. Pubmed Central PMCID: PMC2976880. Epub 2008/05/01. eng.
42. Chu C, Tong SS, Xu Y, Wang L, Fu M, Ge YR, *et al*. Proliposomes for oral delivery of dehydrosilymarin: preparation and evaluation in vitro and in vivo. Acta Pharmacol Sin. 2011;32:973–80. United States.
43. Lu T, Ma Y, Hu H, Chen Y, Zhao W, Chen T. Ethinylestradiol liposome preparation and its effects on ovariectomized rats' osteoporosis. Drug Deliv. 2011;18(7):468–77. PubMed PMID: 21688973. Epub 2011/06/22. eng.
44. Mukherjee S, Ray S, Thakur RS. Solid lipid nanoparticles: a modern formulation approach in drug delivery system. Indian J Pharm Sci. 2009;71(4):349–58. PubMed PMID: 20502539. Pubmed Central PMCID: PMC2865805. Epub 2010/05/27. eng.
45. Roth M. Fluorescence reaction for amino acids. Anal Chem. 1971;43(7):880–2. PubMed PMID: 5576608. Epub 1971/06/01. eng.
46. Dominguez LM, Dunn RS. Analysis of OPA-derivatized amino sugars in tobacco by high-performance liquid chromatography with fluorimetric detection. J Chromatogr Sci. 1987;25(10):468–71. PubMed PMID: 3667835. Epub 1987/10/01. eng.
47. Chen SY, Collipp PJ, Boasi LH, Isenschmid DS, Verolla RJ, Sanroman GA, *et al*. Fluorometry of selenium in human-hair, urine and blood—a single-tube process for sub-microgram

determination of selenium. Ann Nutr Metab. 1982;26(3):186–90. PubMed PMID: WOS:A1982NX76600006. English.
48. Allaway WH, Cary EE. Determination of submicrogram amounts of selenium in biological materials. Anal Chem. 1964;36(7):1359–62.
49. Akinbami LJ, Moorman JE, Garbe PL, Sondik EJ. Status of Childhood Asthma in the United States, 1980–2007. Pediatrics. 2009 Mar;123:S131-S45. PubMed PMID: WOS:000263826000002.
50. Carneiro MFH, Rhoden CR, Amantea SL, Barbosa F. Low concentrations of selenium and zinc in nails are associated with childhood asthma. Biol Trace Elem Res. 2011;144(1–3):244–52. PubMed PMID: WOS:000298192900024.
51. Guo CH, Liu PJ, Hsia S, Chuang CJ, Chen PC. Role of certain trace minerals in oxidative stress, inflammation, CD4/CD8 lymphocyte ratios and lung function in asthmatic patients. Ann Clin Biochem. 2011;48:344–51. England.
52. Yan L, Johnson LK. Selenium bioavailability from naturally produced high-selenium peas and oats in selenium-deficient rats. J Agric Food Chem. 2011;59(11):6305–11. PubMed PMID: 21553810. Epub 2011/05/11. eng.
53. Hambidge KM. Micronutrient bioavailability: dietary reference intakes and a future perspective. Am J Clin Nutr. 2010;91:1430S–2S. United States.
54. Cases J, Wysocka IA, Caporiccio B, Jouy N, Besancon P, Szpunar J, *et al*. Assessment of selenium bioavailability from high-selenium spirulina subfractions in selenium-deficient rats. J Agric Food Chem. 2002;50(13):3867–73. PubMed PMID: WOS:000176267800039.
55. Plano D, Baquedano Y, Ibanez E, Jimenez I, Palop JA, Spallholz JE, *et al*. Antioxidant-prooxidant properties of a new organoselenium compound library. Molecules. 2010;15:7292–312. Switzerland.
56. von Rosen L, Podjaski B, Bettmann I, Otto HF. Observations on the ultrastructure and function of the so-called "microfold" or "membraneous" cells (M cells) by means of peroxidase as a tracer. Virchows Arch A Pathol Anat Histol. 1981;390(3):289–312. PubMed PMID: 7281480. Epub 1981/01/01. eng.
57. Fujimura Y. Functional morphology of microfold cells (M cells) in Peyer's patches—phagocytosis and transport of BCG by M cells into rabbit Peyer's patches. Gastroenterol Jpn. 1986;21(4):325–35. PubMed PMID: 3770353. Epub 1986/08/01. eng.
58. Gupta PN, Vyas SP. Investigation of lectinized liposomes as M-cell targeted carrier-adjuvant for mucosal immunization. Colloids Surf B Biointerfaces. 82. Netherlands: 2010 Elsevier B.V; 2011. p. 118–25.
59. Hsieh EH, Lo DD. Jagged1 and Notch1 help edit M cell patterning in Peyer's patch follicle epithelium. Dev Comp Immunol. 37. United States: 2012 Elsevier Ltd; 2012. p. 306–12.
60. Jepson MA, Simmons NL, Savidge TC, James PS, Hirst BH. Selective binding and transcytosis of latex microspheres by rabbit intestinal M-cells. Cell Tissue Res. 1993;271(3):399–405. PubMed PMID: WOS:A1993KR83100002.
61. Clark MA, Blair H, Liang L, Brey RN, Brayden D, Hirst BH. Targeting polymerised liposome vaccine carriers to intestinal M cells. Vaccine. 2001;20(1–2):208–17. PubMed PMID: WOS:000171512000031. English.
62. Pukanud P, Peungvicha P, Sarisuta N. Development of mannosylated liposomes for bioadhesive oral drug delivery via M cells of Peyer's patches. Drug Deliv. 2009;16(5):289–94. PubMed PMID: WOS:000268575100009. English.
63. Immordino ML, Dosio F, Cattel L. Stealth liposomes: review of the basic science, rationale, and clinical applications, existing and potential. Int J Nanomed. 2006;1(3):297–315. PubMed PMID: 17717971. Pubmed Central PMCID: PMC2426795. Epub 2007/08/28. eng.
64. Shoji Y, Nakashima H. Nutraceutics and delivery systems. J Drug Target. 2004;12:385–91. England.
65. Gomez-Hens A, Fernandez-Romero JM. Analytical methods for the control of liposomal delivery systems. Trac-Trends Anal Chem. 2006;25(2):167–78. PubMed PMID: WOS:000235414500015.
66. Mozafari MR, Johnson C, Hatziantoniou S, Demetzos C. Nanoliposomes and their applications in food nanotechnology. J Liposome Res. 2008;18:309–27. United States.
67. Mozafari MR. Nanoliposomes: preparation and analysis. Meth Mol Biol. 2010;605:29–50. PubMed PMID: 20072871. Epub 2010/01/15. eng.
68. Mozafari MRM, Mortazavi SM. Nanoliposomes: from fundamentals to recent developments. Oxford, UK: Trafford; 2005.
69. Hauser H. Mechanism of spontaneous vesiculation. Proc Natl Acad Sci U S A. 1989;86(14):5351–5. Pubmed Central PMCID: PMC297620. Epub 1989/07/01. eng.
70. Mura P, Maestrelli F, Gonzalez-Rodriguez ML, Michelacci I, Ghelardini C, Rabasco AM. Development, characterization and in vivo evaluation of benzocaine-loaded liposomes. Eur J Pharm Biopharm. 2007;67:86–95. Netherlands.
71. Colas JC, Shi W, Rao VS, Omri A, Mozafari MR, Singh H. Microscopical investigations of nisin-loaded nanoliposomes prepared by Mozafari method and their bacterial targeting. Micron. 2007;38:841–7. England.
72. Girod de Bentzmann S, Pierrot D, Fuchey C, Zahm JM, Morancais JL, Puchelle E. Distearoyl phosphatidylglycerol liposomes improve surface and transport properties of CF mucus. Eur Respir J. 1993;6(8):1156–61. PubMed PMID: 8224130. Epub 1993/09/01. eng.
73. Metselaar JM, Bruin P, de Boer LW, de Vringer T, Snel C, Oussoren C, *et al*. A novel family of L-amino acid-based biodegradable polymer-lipid conjugates for the development of long-circulating liposomes with effective drug-targeting capacity. Bioconjugate Chem. 2003;14(6):1156–64. PubMed PMID: 14624629. Epub 2003/11/20. eng.
74. Deniz A, Sade A, Severcan F, Keskin D, Tezcaner A, Banerjee S. Celecoxib-loaded liposomes: effect of cholesterol on encapsulation and in vitro release characteristics. Biosci Rep. 2010;30:365–73. United States.
75. Berg J, Tymoczko JL, Stryer L. Section 12.3, There are three common types of membrane lipids. Biochemistry. 2002.
76. Wu Y, Ho YP, Mao Y, Wang X, Yu B, Leong KW, *et al*. Uptake and intracellular fate of multifunctional nanoparticles: a comparison between lipoplexes and polyplexes via quantum dot mediated Forster resonance energy transfer. Mol Pharm. 2011;8(5):1662–8. PubMed PMID: 21740056. Pubmed Central PMCID: PMC3185110. Epub 2011/07/12. eng.
77. Elder A, Vidyasagar S, DeLouise L. Physicochemical factors that affect metal and metal oxide nanoparticle passage across epithelial barriers. Wiley Interdiscip Rev Nanomed Nanobiotechnol. 2009;1(4):434–50. PubMed PMID: 20049809. Epub 2010/01/06. eng.
78. Ponchel G, Irache J. Specific and non-specific bioadhesive particulate systems for oral delivery to the gastrointestinal tract. Adv Drug Deliv Rev. 1998;34:191–219.
79. Toy R, Hayden E, Shoup C, Baskaran H, Karathanasis E. The effects of particle size, density and shape on margination of nanoparticles in microcirculation. Nanotechnology. 2011;22(11):115101. PubMed PMID: 21387846. Epub 2011/03/11. eng.
80. Paliwal R, Paliwal SR, Mishra N, Mehta A, Vyas SP. Engineered chylomicron mimicking carrier emulsome for lymph targeted oral delivery of methotrexate. Int J Pharm. 2009;380(1–2):181–8. PubMed PMID: WOS:000270495400025.
81. Allen TM, Hansen C. Pharmacokinetics of stealth versus conventional liposomes—effect of dose. Biochimica Et Biophysica Acta. 1991;1068(2):133–41. PubMed PMID: WOS:A1991GL84200003.
82. Nicholas TE, Barr HA, Power JH, Jones ME. Uptake of instilled radiolabeled lamellar bodies from alveolar compartment of the rat. Am J Physiol. 1990;259(4 Pt 1):L238–46. PubMed PMID: 2221085. Epub 1990/10/01. eng.
83. Tagami T, May JP, Ernsting MJ, Li SD. A thermosensitive liposome prepared with a Cu2+ gradient demonstrates improved pharmacokinetics, drug delivery and antitumor efficacy. J Contr Release. 2012;161(1):142–9. PubMed PMID: WOS:000305790100016.
84. Ganta S, Deshpande D, Korde A, Amiji M. A review of multifunctional nanoemulsion systems to overcome oral and CNS drug delivery barriers. Mol Membr Biol. 2010;27(7):260–73. PubMed PMID: 20929336. Epub 2010/10/12. eng.
85. Gerasimov OV, Boomer JA, Qualls MM, Thompson DH. Cytosolic drug delivery using pH- and light-sensitive liposomes. Adv Drug Deliv Rev. 1999;38:317–38.
86. Lentz BR, Lee JK. Poly(ethylene glycol) (PEG)-mediated fusion between pure lipid bilayers: a mechanism in common with viral fusion and secretory vesicle release? Mol Membr Biol. 1999;16(4):279–96. PubMed PMID: 10766128. Epub 2000/04/15. eng.
87. Lee SJ, Schlesinger PH, Wickline SA, Lanza GM, Baker NA. Simulation of fusion-mediated nanoemulsion interactions with

model lipid bilayers. Soft Matter. 2012;8(26):3024–35. PubMed PMID: 22712024. Pubmed Central PMCID: PMC3375911. Epub 2012/06/20. Eng.
88. Bloom M, Evans E, Mouritsen OG. Physical properties of the fluid lipid-bilayer component of cell membranes: a perspective. Q Rev Biophys. 1991;24(3):293–397. PubMed PMID: 1749824. Epub 1991/08/01. eng.
89. Virden JW, Berg JC. NACL-induced aggregation of dipalmitoylphosphatidylglycerol small unilamellar vesicles with varying amounts of incorporated cholesterol. Langmuir. 1992;8(6):1532–7. PubMed PMID: WOS:A1992JA58300007.
90. Mayer LD, Bally MB, Hope MJ, Cullis PR. Uptake of antineoplastic agents into large unilamellar vesicles in response to a membrane potential. Biochim Biophys Acta. 1985;816(2):294–302. PubMed PMID: 3839135. Epub 1985/06/27. eng.
91. Mayhew E, Rustum YM, Szoka F, Papahadjopoulos D. Role of cholesterol in enhancing the antitumor activity of cytosine arabinoside entrapped in liposomes. Cancer Treat Rep. 1979;63(11–12):1923–8. PubMed PMID: 526925. Epub 1979/11/01. eng.
92. Dos Santos N, Mayer LD, Abraham SA, Gallagher RC, Cox KA, Tardi PG, *et al*. Improved retention of idarubicin after intravenous injection obtained for cholesterol-free liposomes. Biochim Biophys Acta. 2002;1561:188–201. Netherlands.
93. Taira MC, Chiaramoni NS, Pecuch KM, Alonso-Romanowski S. Stability of liposomal formulations in physiological conditions for oral drug delivery. Drug Deliv. 2004;11:123–8. England.
94. Vasconcelos T, Sarmento B, Costa P. Solid dispersions as strategy to improve oral bioavailability of poor water soluble drugs. Drug Discov Today. 2007;12:1068–75. England.
95. Castelli F, Puglia C, Sarpietro MG, Rizza L, Bonina F. Characterization of indomethacin-loaded lipid nanoparticles by differential scanning calorimetry. Int J Pharm. 2005;304:231–8. Netherlands.
96. Simon SL. Temperature-modulated differential scanning calorimetry: theory and application. Thermochim Acta. 2001;374(1):55–71. PubMed PMID: WOS:000171624700008.
97. Bunjes H, Unruh T. Characterization of lipid nanoparticles by differential scanning calorimetry, X-ray and neutron scattering. Adv Drug Deliv Rev. 2007;59(6):379–402. PubMed PMID: WOS:000249543300003.
98. Aburahma MH, Abdelbary GA. Novel diphenyl dimethyl bicarboxylate provesicular powders with enhanced hepatocurative activity: preparation, optimization, in vitro/in vivo evaluation. International Journal of Pharmaceutics. Netherlands: 2011 Elsevier B.V; 2012. 422:139–50.
99. Hancock BC, Morris KR, Wildfong PL. A priori performance predictions in the pharmaceutical sciences. Int J Pharm. 2011;418:149–50. Netherlands.
100. Jepson MA, Clark MA, Hirst BH. M cell targeting by lectins: a strategy for mucosal vaccination and drug delivery. Adv Drug Deliv Rev. 2004;56:511–25. Netherlands.
101. Zhang N, Ping QN, Huang GH, Xu WF. Investigation of lectin-modified insulin liposomes as carriers for oral administration. Int J Pharm. 2005;294:247–59. Netherlands.
102. Wagner S, Lynch NJ, Walter W, Schwaeble WJ, Loos M. Differential expression of the murine mannose-binding lectins A and C in lymphoid and nonlymphoid organs and tissues. J Immunol. 2003;170(3):1462–5. PubMed PMID: 12538708. Epub 2003/01/23. eng.
103. Ermak TH, Giannasca PJ. Microparticle targeting to M cells. Adv Drug Deliv Rev. 1998;34:261–83.
104. Palumbo RN, Wang C. Bacterial invasin: structure, function, and implication for targeted oral gene delivery. Curr Drug Deliv. 2006;3(1):47–53. PubMed PMID: 16472093. Epub 2006/02/14. eng.
105. Hoffmann PR, Jourdan-Le Saux C, Hoffmann FW, Chang PS, Bollt O, He Q, *et al.* A role for dietary selenium and selenoproteins in allergic airway inflammation. J Immunol. 2007;179:3258–67. United States.